

## Aligned wet-electrospun starch fiber mats

Hui Wang – Pennsylvania State University

Lingyan Kong – University of Alabama

Gregory R. Ziegler – Pennsylvania State  
University

Deposited 04/28/2020

Citation of published version:

Wang, H., Kong, L., Ziegler, G. (2019): Aligned wet-electrospun starch fiber mats. *Food Hydrocolloids*, vol. 90.

DOI: <https://doi.org/10.1016/j.foodhyd.2018.12.008>



Full text at <https://doi.org/10.1016/j.foodhyd.2018.12.008>

or send request to [lingyan.kong@ua.edu](mailto:lingyan.kong@ua.edu)

## **Aligned wet-electrospun starch fiber mats**

Hui Wang<sup>a</sup>, Lingyan Kong<sup>b</sup>, and Gregory R. Ziegler<sup>a,\*</sup>

<sup>a</sup> Department of Food Science, Pennsylvania State University, University Park, Pennsylvania 16802, United States

<sup>b</sup> Department of Human Nutrition and Hospitality Management, The University of Alabama, Tuscaloosa, Alabama 35487, United States

For submission to: *Food Hydrocolloids Special 14IHC Edition*

\* Corresponding author. Tel.: +1 814 863 2960; fax: +1 814 863 6132. E-mail address: [grz1@psu.edu](mailto:grz1@psu.edu). Address: 341 Rodney A. Erickson Food Science Building University Park, PA 16802.

Abstract:

Electrospinning is a versatile technique to fabricate non-woven fiber mats with an average fiber diameter ranging from nanometers to micrometers. Fibers produced by electrospinning have potential application in numerous fields owing to their light weight, high surface area, and high porosity. In certain applications, anisotropic properties are desired, which may also improve mechanical strength. This study comprehensively documented the feasibility of directed fiber deposition in wet-electrospinning and offers an inexpensive setup for laboratory investigation. Aligned starch fiber mats were produced and the effects of three operational parameters, i.e., rotational speed, drum location, and coagulation bath composition, were evaluated. The alignment of starch fibers was affected by the ethanol concentration in the coagulation bath and drum rotational speed. Coherent fibers could be obtained in all trials except for the one at the lowest ethanol concentration (60% v/v) and highest rotational speed (500 rpm) when the drum was below the liquid. The tensile strength was influenced by the interaction of location and ethanol concentration, and that of rotational speed and ethanol concentration. This study set a promising example of making aligned biopolymer fiber mats and investigating fiber deposition in wet-electrospinning. Aligned starch fiber mats have potential applications in areas such as tissue engineering and as wound dressings.

Keywords (6 keywords): starch fiber mat, wet-electrospinning, drum drawing, tensile strength, aligned fiber, fiber orientation

## **1. Introduction:**

Electrospinning is a versatile technique to fabricate non-woven fibers with an average diameter ranging from nanometers to micrometers. A basic electrospinning setup consists of a spinning dope reservoir, pump, spinneret, high voltage source, and grounded collector. The spinning dope is pumped through the spinneret, where the surface of the extruded droplet becomes charged and is stretched towards the grounded collector in the electric field gradient. In dry-electrospinning the solvent evaporates during elongation leaving a dry fiber. In wet-electrospinning, the solvent is extracted in a coagulation bath containing a non-solvent, precipitating the polymer, and resulting in fiber formation.

Fibers produced by electrospinning have potential application in numerous fields owing to their light weight, high surface area, and high porosity. In applications such as biomedical materials and microelectronics anisotropic properties, i.e., oriented fibers, are desired. For example, aligned fiber mats mimic natural extracellular matrices (ECM) and facilitate cell adhesion, growth, and proliferation (Choi, Lee, Christ, Atala, & Yoo, 2008; Vimal, Ahamad, & Katti, 2016). Aligned or oriented fibers may also possess superior uniaxial mechanical properties compared to their randomly oriented counterparts. In addition, the diameter of aligned fibers is usually reduced during the alignment procedure (Afifi, Nakajima, Yamane, Kimura, & Nakano, 2009; Lee & Deng, 2012). Therefore, fiber alignment is a strategy for developing electrospun fibers with enhanced functionality.

Methods to achieve and control fiber alignment in dry-electrospinning have been summarized in a series of review articles (Abbasipour & Khajavi, 2013; Baji, Mai, Wong, Abtahi, & Chen, 2010; Ner, Asemota, Olson, & Sotzing, 2009; Sahay, Thavasi, & Ramakrishna, 2011). Fiber alignment in dry-electrospinning can be achieved by modifying the collector or

using auxiliary electrodes. Various types of collectors, including drum/mandrel/rotator, disk, hollow drum, and rotating ‘funnel’ target, have been used to align electrospun fibers (Afifi, Nakano, Yamane, & Kimura, 2010). Using a rotating drum as the grounded collector seems to be the most practical way to align electrospun fibers due to its simplicity and versatility. Increasing the speed of drum rotation (or surface velocity) up to a critical level often resulted in greater fiber orientation or alignment (Fennessey & Farris, 2004; Pan, Li, Hu, & Cui, 2006). Fiber breakage often took place above the critical speed (Pan et al., 2006).

Compared to dry-electrospinning, adapting the rotating drum method for fiber alignment in wet-electrospinning is challenging, since there are other influential factors to be considered, e.g., coagulation bath composition, the location of drum relative to the bath surface, and the possibility of bath turbulence caused by high drum rotational speed. Because wet-electrospinning is often used to produce bio-based fibers, including starch fibers (Kong & Ziegler, 2012, 2014), controlling the fiber deposition and alignment in wet-electrospinning is worthy of investigation.

In this project, we assembled an inexpensive, easily reconfigurable rotating drum collector to align fibers produced by wet-electrospinning, and addressed the influence of key parameters, including coagulation bath composition, drum position relative to the bath surface, and drum rotational speed, on fiber alignment. We hypothesized that increasing drum rotational speed within a certain range would increase the degree of fiber orientation. We varied the ethanol and water composition in the coagulation bath. We hypothesized that as the water fraction increased, a higher degree of fiber orientation and smaller fiber diameter would result due to slower fiber coagulation and solidification. Unique to wet-electrospinning, we expected that the location of the drum in the coagulation bath would influence the drawing effect and the solidification of the polymer jet, and thus affect fiber diameter and alignment.

## **2. Materials & methods**

### *2.1. Materials*

High amylose maize starch (HAMS, Gelose 80) was kindly supplied by Ingredion (Bridgewater, NJ). Dimethyl sulfide (DMSO) and 200 proof ethanol were purchased from VWR International (Radnor, PA).

### *2.2. Dope preparation*

The electrospinning dope, 12% (w/v) HAMS (Kong & Ziegler, 2013; Wang, Kong, & Ziegler, 2018) dispersion in pure DMSO, was prepared by heating the dispersion in a boiling water bath with continuous stirring for about 1 h.

### *2.3. Electrospinning*

The electrospinning apparatus comprised a high voltage power supply (ES40P, Gamma High Voltage Research, Inc., Ormond Beach, FL), a syringe pump (81620, Hamilton Company, Reno, NV), a 3 mL plastic syringe (Becton, Dickinson and Company, Franklin Lakes, NJ) with a 20-gauge blunt needle (Kong & Ziegler, 2014), and a grounded rotating drum collector (Figure 1). The rotating drum collector was assembled from Lego® parts, including the Lego® Technic Power Functions Motor Set (The Lego Group, Billund, Denmark). The plastic nature of the Lego® system insulated it from the electric field. A filter screen (Model FSS, Presque Isle Wine Cellars, diameter 15.8750 mm, length 53.975 mm) was used as the drum. The speed of the rotating drum was controlled by changing the drive gear ratio. The speeds applied were  $200\pm 10$ ,  $380\pm 10$ , and  $500\pm 10$  rpm (corresponding to surface velocities of 0.165, 0.298, and 0.400 m/s, respectively), and designated as S200, S380 and S500, respectively. A hand-held digital tachometer (DT-205B, SHIMPO America Corp., Lincolnwood, IL) was used to confirm the angular speed of the rotating drum. The composition of the coagulation bath was either 100%,

80%, or 60% (v/v), ethanol in water, denoted E100, E80 and E60, respectively. Two drum positions, either above (A) or below (B) the coagulation bath surface, were tested (Figure 2). The drum position was determined based on a preliminary test, by maximizing the difference in drum position while avoiding extreme bath agitation caused by the drum rotation and changed by altering the bath depth. Wet-electrospinning was carried out at predetermined parameters: positive voltage at 11 kV, spinning distance at 3.5 cm from the spinneret to the top of the drum, and dope flow rate at 10.5 mL/h.

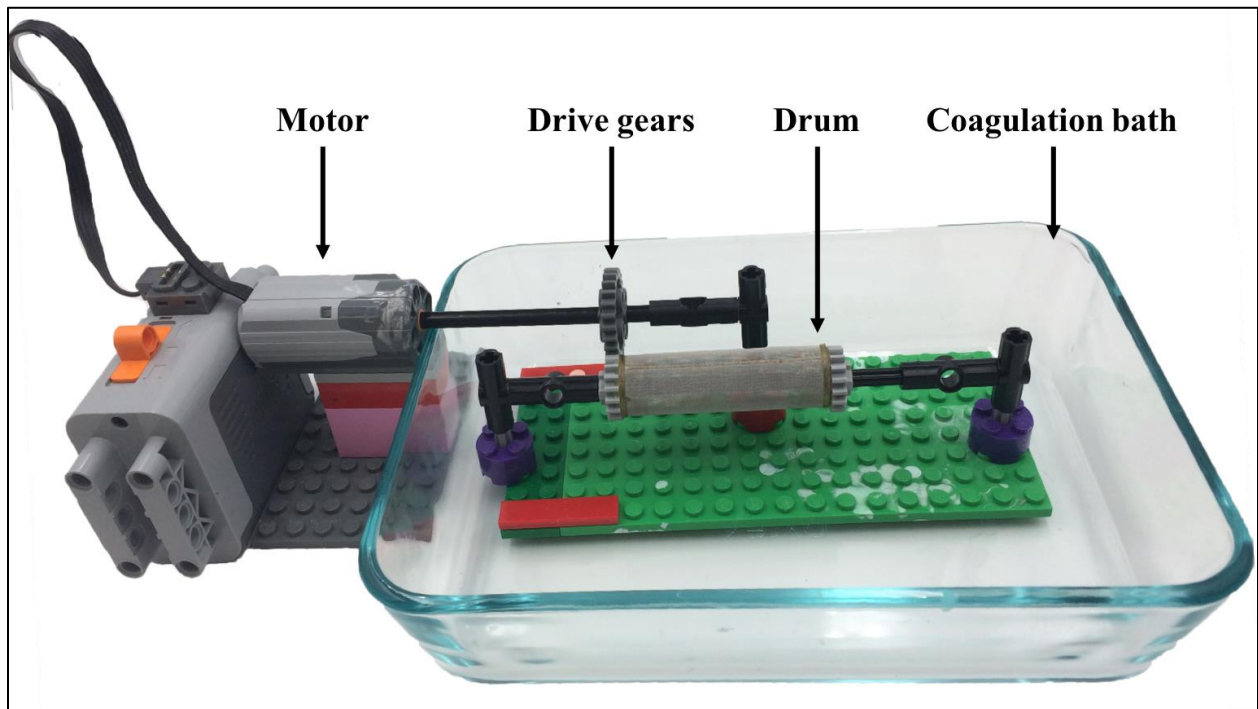


Figure 1. Rotating drum collector setup used to align starch fibers produced by wet-electrospinning.

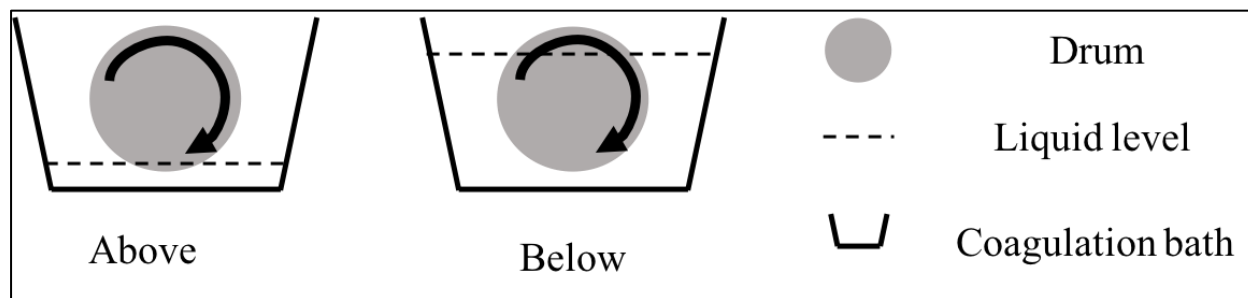


Figure 2. Schematic illustration of the drum location relative to the coagulation bath surface.

#### *2.4. Morphological analysis and quantification of fiber alignment*

Microscopic observation of electrospun starch fibers was performed using a Phenom G2 Pro scanning electron microscope (SEM, Phenom-World, Eindhoven, The Netherlands) at an accelerating voltage of 5 keV. Fiber diameter distributions were evaluated based on at least 8 SEM images using an open source software, ImageJ and Fityk 0.9.8 (Hotaling, Bharti, Kriel, & Simon, 2015; Wang, Kong, & Ziegler, 2018).

The degree of fiber alignment or fiber orientation in starch fiber mats, i.e., fiber orientation distribution (FOD) from  $-90^{\circ}$  to  $90^{\circ}$ , of each SEM image was analyzed using Fourier transform via the OrientationJ plugin in ImageJ. The  $0^{\circ}$  angle corresponded to the horizontal orientation parallel to the drum axis and increased counter-clockwise. The FOD of each SEM image was fitted to the von Mises distribution using Matlab R2017b (Mathworks, Natick, MA) according to Fee, Downs, Eberhardt, Zhou, and Berry (2016). The parameter  $\kappa$  of the von Mises distribution was used to summarize the FOD of each SEM image. The mean  $\kappa$  was calculated for each sample based on at least 7 images.

#### *2.5. Uniaxial tensile test*

Dried fiber mats were equilibrated at 75% relative humidity and  $25^{\circ}\text{C}$  for 1 hour, to prevent fiber damage during peeling and flattening before tensile measurement. After flattening under the weight of 2 microscope slides, each sample (5.3 mm wide and approximately 25 mm long,



parallel to the alignment direction) was cut out using a film cutter (PN 984485.901, TA Instruments, New Castle, DE). The weight of each fiber mat sample was recorded using a Mettler-Toledo XP2U ultra-microbalance (Mettler-Toledo International Inc., Columbus, OH). Uniaxial tension tests were carried out using a Q800 dynamic mechanical analyzer (DMA, TA Instruments, New Castle, DE), with a film tension clamp using controlled force mode at room temperature (20 °C). The controlled force was applied parallel to the aligned direction at a rate of 0.05 N/min, with a preload force of 0.001 N. Weight-normalized ultimate tensile strength (WNUTS) was calculated (Wang et al., 2018). At least two samples for each of two treatment replicates were evaluated.

### *2.6. Statistical analysis*

A 2x3x3 full-factorial, completely randomized block design was applied to investigate the effects of drum location (above or below coagulation bath), rotational speed (S200, S380 and S500) and ethanol concentration in the coagulation bath (E100, E80 and E60) on the tensile properties and FOD, with replication as the block. ANOVA with general linear model (a quadratic model with 2-sided 95% confidence interval and forward stepwise selection with  $\alpha < 0.25$  to retain) was used to analyze the effects of factors, and Tukey's test was used for the mean separation (Minitab 18.1, Minitab, Inc., State College, PA). Missing data were treated as likewise deletion by software default.

## **3. Results and discussion**

### *3.1. Rotating collector design for wet-electrospinning*

Like in dry-electrospinning, the drum should be conductive to serve as a target for fiber accumulation. In addition, a rotating drum collector in wet-electrospinning requires high corrosion resistance, good motor insulation, and minimum bath agitation. We found Lego® parts

are affordable and feasible tools to assemble the rotating drum collector for wet-electrospinning, due to their electrical insulation and easy adjustment.

### *3.2. Electrospinnability*

Drum drawing significantly affected the wet-electrospinnability of starch fibers.

Representative scanning electron micrographs of electrospun starch fiber mats as a function of coagulation bath composition, speed of drum rotation, and drum collector position, are shown in Figures 3 and 4. Starch fiber mats were successfully collected on the rotating drum in all experimental conditions except for the E60-S500-B trial, i.e., when the drum was positioned below the surface of the coagulation bath containing 60% (v/v) ethanol, the fibers broke at the highest rotational speed and could not be collected on the drum. We have previously shown that pure starch fibers could be successfully fabricated using a coagulation bath with aqueous ethanol concentrations varying from 60% to 100% (v/v) (Kong & Ziegler, 2014). Fiber formation in wet-electrospinning depends on the diffusion of the dope solvent to the coagulation bath (Yi et al., 2013) and precipitation of the solid fiber. A lower ethanol content would slow the diffusion of DMSO from the fibers and decrease the rate of precipitation, resulting in a slower solidification of the starch fiber mats. Consequently, as the drum rotational speed increased these not fully solidified and fragile fibers were broken and no coherent fiber mat was collected on the rotating drum.

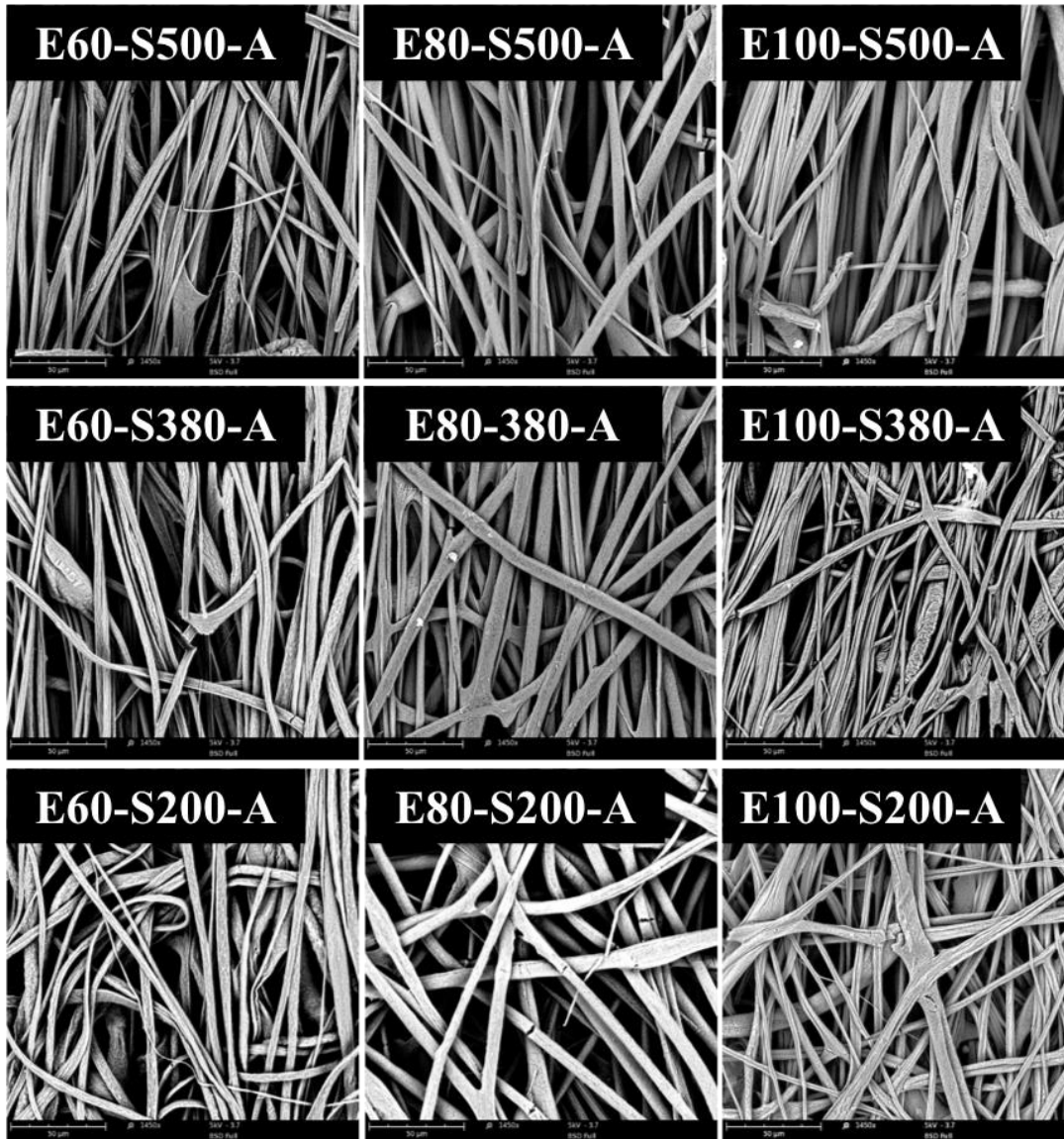


Figure 3. Scanning electron microscopy images of high-amylose starch fiber mats spun with the collector drum above the coagulation bath. Ethanol concentration and the rotational speed are indicated in the legends.

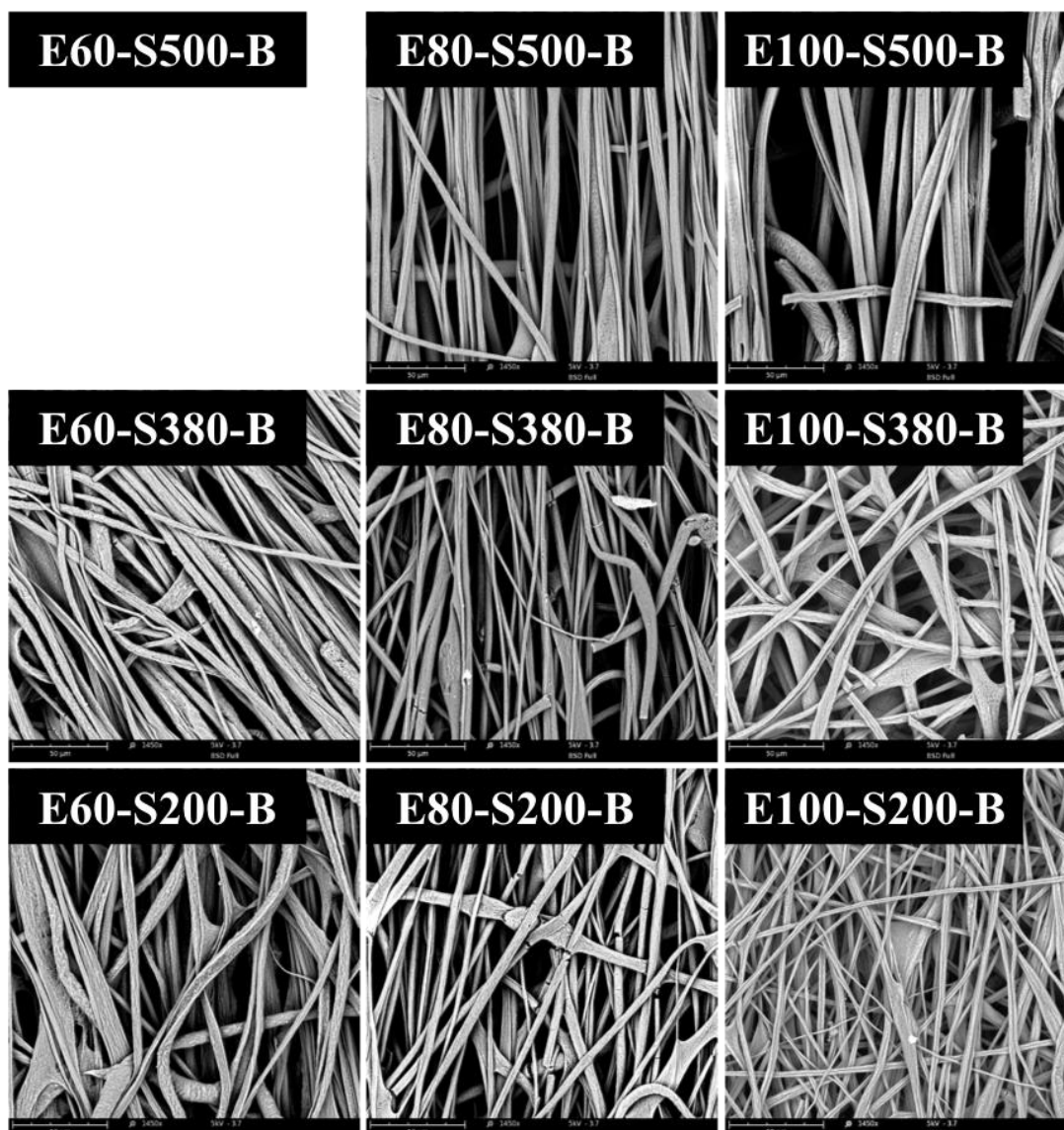


Figure 4. Scanning electron microscopy images of high-amylose starch fiber mats with the collector drum below the coagulation bath. Ethanol concentration and the rotational speed are indicated in the legends.

### 3.3. Fiber diameter and alignment

Fiber diameter, fiber alignment, and their distributions were obtained from SEM images (similar to Figures 3 & 4). Consistent with our previous studies on starch fiber mats (Kong &

Ziegler, 2013; Wang et al., 2018), the mean starch fiber diameters fell into a narrow range between 2.15  $\mu\text{m}$  and 4.02  $\mu\text{m}$ . The experimental factors had no significant influence on fiber diameter (Table 1). Several investigators reported an influence of drum drawing on fiber diameter in dry electrospinning. For example, the average diameter of electrospun cellulose nano-whiskers/poly(vinyl alcohol) fibers (Lee & Deng, 2012) and poly(L-lactide) fibers (Afifi et al., 2009) decreased with increasing drum rotational speed. However, other studies found the average fiber diameter was not affected by drum drawing. For instance, the average diameter of poly( $\epsilon$ -caprolactone)/collagen nanofibers was not significantly influenced by the rotational speed of the drum (Choi et al., 2008). The diameter of electrospun fibers is governed largely by jet elongation under the influence of electric and viscous forces (Narayanan, Tekbudak, Caydamli, Dong, & Krause, 2017; Stepanyan et al., 2014). Mechanical drawing is only possible while the fiber is still compliant. Whether the rotational speed has an impact on fiber diameter depends on the electrospinning method and the fiber material. In wet-electrospinning the drum is covered by a liquid layer. Therefore, fibers may not adhere as readily to the drum on initial contact and, hence the draw ratio, i.e., the ratio of the final fiber length to the initial length, in wet-electrospinning might be less than that in dry-electrospinning.

Table 1. Electrospinning conditions, fiber dimensions, weight normalized ultimate tensile strength (WNUTS) and kappa value for each treatment combination.

Ethanol concentration v/v %	Rotation rpm	Drum location	WNUTS* N/g	Fiber diameter $\mu\text{m}$	Kappa
60	200	Above	13.55±0.85 <sup>c</sup>	2.22±0.04	2.43±1.96
60	200	Below	18.48±10.06 <sup>c</sup>	2.42±0.27	2.52±0.17
60	380	Above	32.14±13.65 <sup>bc</sup>	2.42±0.43	2.69±0.32
60	380	Below	18.84±5.61 <sup>bc</sup>	2.44±0.08	3.27±0.05
60	500	Above	65.75±9.63 <sup>ab</sup>	2.30±0.08	3.47±1.34
60	500	Below	-	-	-
80	200	Above	15.24±8.09 <sup>bc</sup>	3.06±1.04	1.32±0.42
80	200	Below	40.99±29.41 <sup>bc</sup>	2.33±0.10	1.36±0.28
80	380	Above	27.12±2.28 <sup>bc</sup>	3.15±0.90	2.09±0.30
80	380	Below	38.81±5.02 <sup>bc</sup>	2.39±0.46	2.43±1.29
80	500	Above	55.24±10.99 <sup>a</sup>	2.36±0.71	3.28±0.44
80	500	Below	87.74±1.70 <sup>a</sup>	3.17±1.49	6.15±2.85
100	200	Above	68.35±7.10 <sup>ab</sup>	2.30±0.17	2.00±0.32
100	200	Below	40.68±6.27 <sup>ab</sup>	2.33±0.10	1.82±0.24
100	380	Above	66.86±19.00 <sup>ab</sup>	2.31±0.91	1.64±1.26
100	380	Below	33.54±10.34 <sup>ab</sup>	4.02±2.36	1.17±0.54
100	500	Above	71.36±26.65 <sup>ab</sup>	2.31±0.09	2.03±0.03
100	500	Below	26.74±0.26 <sup>ab</sup>	2.15±0.14	2.81±1.02

\* Means that do not share a letter in common are significantly different using Tukey's

method ( $\alpha=0.05$ ).

The draw ratio is proportional to the ratio of the final fiber velocity to the initial jet velocity (Fennessey & Farris, 2004). A higher draw ratio is preferred to reduce fiber diameter. The velocity of the electrospinning jet ranges from 2 m/s to 186 m/s (Teo & Ramakrishna, 2006). To reduce the fiber diameter, the linear velocity of the rotating drum needs to be faster than the velocity of the jet, which was difficult to achieve in this wet-electrospinning setup, since to avoid liquid splashing rotational speeds were limited. The highest rotational speed attained in this study was 0.4 m/s, which may not be sufficient to reduce the starch fiber diameter. A larger diameter drum could be used to increase the linear velocity in future experiments.

Although the rotating drum collector was not capable of drawing the fibers to a finer size, progressive increase in fiber alignment was observed as the rotational speed increased (Figures 3 and 4). When the degree of fiber alignment, quantified by the parameter  $\kappa$ , is close to 0, the distribution of fiber orientation is random in all directions; as  $\kappa$  becomes larger, the fibers are oriented with a preference at a certain angle (Fee et al., 2016). The main factors of ethanol concentration, rotational speed and replication (block factor) had significant ( $\alpha < 0.05$ ) influence on fiber alignment (Table 2). The factor location was nearly significant ( $p = 0.057$ ) as were the interactions among factors ( $p = 0.066$  &  $0.078$ ). A lower ethanol concentration resulted in a higher  $\kappa$ , indicating a better alignment. Lower ethanol concentrations reduce the fiber solidification rate, permitting greater time for fiber alignment. The influence of high rotational speed on fiber alignment is in agreement with the phenomenon in dry-electrospinning, where higher rotational speed introduced better fiber alignment (Fee et al., 2016; Fennessey & Farris, 2004).

Table 2. Analysis of variance table for kappa\*.

Analysis of Variance					
Source	DF	Adj SS	Adj MS	F-Value	P-Value
Location	1	3.277	3.2772	4.07	0.057
Ethanol	2	9.738	4.8692	6.05	0.008
Rotational speed	2	19.535	9.7676	12.13	0.000
Block	1	5.098	5.0977	6.33	0.02
Location*rotational speed	2	4.662	2.3308	2.9	0.078
Ethanol*rotational speed	4	8.332	2.083	2.59	0.066
Error	21	16.905	0.805		
Total	33	63.025			

\*Forward stepwise selection starts with an empty model and adds the most significant term for each step till all variables not in the model have p-values greater than  $\alpha = 0.25$ .

### 3.4. Tensile strength of fiber mat

To evaluate tensile strength of the aligned starch fiber mats, weight-normalized ultimate tensile strength (WNUTS) was measured (Table 1). The WNUTS values range from 13.55 to 87.74 N/g among all treatments. The maximum WNUTS of fiber mats was observed for the E80-S500-B trial. Table 3 shows the effects of ethanol on WNUTS depended on drum location and rotational speed. Despite the location of the drum, WNUTS increased as the rotational speed increased for ethanol concentrations of 60% and 80%. The influence of rotational speed on WNUTS was not significant when ethanol concentration was 100% (Table 1). At the same rotational speed, fiber mats were stronger when the drum was above the liquid for ethanol concentrations of 60% and 100%.

Table 3. Analysis of variance table for weight normalized tensile stress (WNUTS)\*.

Analysis of variance					
Source	DF	Adj SS	Adj MS	F-Value	P-Value
Location	1	221.6	221.6	1.48	0.237
Ethanol	2	1262	631	4.2	0.029
Rotational speed	2	4392	2196	14.62	0.000
Location*Ethanol	2	5140.6	2570.3	17.11	0.000
Ethanol*Rotational speed	4	3426.9	856.7	5.7	0.003
Error	22	3305.3	150.2		
Total	33	19270.9			

\*Forward stepwise selection starts with an empty model and adds the most significant term for each step till all variables not in the model have p-values greater than  $\alpha=0.25$ .

An increase in tensile strength attributable to fiber alignment is consistent with previous reports on the effect of drum drawing on tensile properties of fiber mats from dry-electrospinning (Choi et al., 2008; Fee et al., 2016). Uniaxially aligned fiber mats were found to promote an equal distribution of tensile force to all fibers along the fiber alignment direction.



#### **4. Conclusion**

In conclusion, aligned starch fiber mats were made by wet-electrospinning equipped with an inexpensive custom-made rotating drum collector. The influence of selected parameters (rotational speed, coagulation bath composition, and drum location) on fiber formation, alignment, and tensile strength were examined. Smooth fibers could be obtained in all trials except for the E60-S500-B trial. The alignment of starch fibers was affected by the ethanol concentration in the coagulation bath and drum rotational speed. In general, higher rotational speed and lower ethanol concentration facilitated better fiber alignment. The tensile strength was correlated with fiber alignment and affected by the location-ethanol concentration interaction and rotational speed-ethanol concentration interaction. The condition to reach the best fiber alignment and maximize WNUTS of the fiber mats was determined to be the E80-S500-B trial. Under current conditions, fiber diameter at macro scale was not reduced by drum drawing, and the improvement in tensile strength is mainly due to the fiber alignment. This study set a promising example of making aligned biopolymer fiber mats and investigating fiber deposition in wet-electrospinning. Utilizing oriented starch fiber mats in applications such as tissue engineering and wound dressing can be explored.

## **Acknowledgements**

This project is funded by the USDA National Institute for Food and Agriculture, Agriculture and Food Research Initiative Program, Competitive Grants Program award from the Nanotechnology for Agricultural and Food Systems (A1511) program FY 2014 as grant # 2015-67021-22994.

## Reference

- Abbasipour, M., & Khajavi, R. (2013). Nanofiber bundles and yarns production by electrospinning: A review. *Advances in Polymer Technology*, 32(3), 1–9.
- Afifi, A. M., Nakajima, H., Yamane, H., Kimura, Y., & Nakano, S. (2009). Fabrication of aligned poly(L-lactide) fibers by electrospinning and drawing. *Macromolecular Materials and Engineering*, 294(10), 658–665.
- Baji, A., Mai, Y. W., Wong, S. C., Abtahi, M., & Chen, P. (2010). Electrospinning of polymer nanofibers: Effects on oriented morphology, structures and tensile properties. *Composites Science and Technology*, 70(5), 703–718.
- Choi, J. S., Lee, S. J., Christ, G. J., Atala, A., & Yoo, J. J. (2008). The influence of electrospun aligned poly( $\epsilon$ -caprolactone)/collagen nanofiber meshes on the formation of self-aligned skeletal muscle myotubes. *Biomaterials*, 29(19), 2899–2906.
- Fee, T., Downs, C., Eberhardt, A., Zhou, Y., & Berry, J. (2016). Image-based quantification of fiber alignment within electrospun tissue engineering scaffolds is related to mechanical anisotropy. *Journal of Biomedical Materials Research - Part A*, 104(7), 1680–1686.
- Fennessey, S. F., & Farris, R. J. (2004). Fabrication of aligned and molecularly oriented electrospun polyacrylonitrile nanofibers and the mechanical behavior of their twisted yarns. *Polymer*, 45(12), 4217–4225.
- Hotaling, N. A., Bharti, K., Kriel, H., & Simon, C. G. (2015). DiameterJ: A validated open source nanofiber diameter measurement tool. *Biomaterials*, 61, 327–338.
- Kong, L., & Ziegler, G. R. (2012). Patents on fiber spinning from starches. *Recent Patents on Food, Nutrition & Agriculture*, 4(3), 210–219.
- Kong, L., & Ziegler, G. R. (2013). Quantitative relationship between electrospinning parameters and starch fiber diameter. *Carbohydrate Polymers*, 92(2), 1416–1422.
- Kong, L., & Ziegler, G. R. (2014). Fabrication of pure starch fibers by electrospinning. *Food Hydrocolloids*, 36, 20–25.
- Lee, J., & Deng, Y. (2012). Increased mechanical properties of aligned and isotropic electrospun PVA nanofiber webs by cellulose nanowhisker reinforcement. *Macromolecular Research*, 20(1), 76–83.
- Narayanan, G., Tekbudak, M. Y., Caydamli, Y., Dong, J., & Krause, W. E. (2017). Accuracy of electrospun fiber diameters: The importance of sampling and person-to-person variation. *Polymer Testing*, 61, 240–248.
- Ner, Y., Asemota, C., Olson, J. R., & Sotzing, G. A. (2009). Nanofiber alignment on a flexible substrate: hierarchical order from macro to nano. *ACS Applied Materials & Interfaces*, 1(10), 2093–2097.
- Pan, H., Li, L., Hu, L., & Cui, X. (2006). Continuous aligned polymer fibers produced by a modified electrospinning method. *Polymer*, 47(14), 4901–4904.
- Sahay, R., Thavasi, V., & Ramakrishna, S. (2011). Design modifications in electrospinning setup for advanced applications. *Journal of Nanomaterials*, 2011, 1–17.
- Stepanyan, R., Subbotin, A., Cuperus, L., Boonen, P., Dorschu, M., Oosterlinck, F., & Bulters, M. (2014). Fiber diameter control in electrospinning. *Applied Physics Letters*, 105(10), 173105–2201.
- Teo, W. E., & Ramakrishna, S. (2006). A review on electrospinning design and nanofibre assemblies. *Nanotechnology*, 17(14), R89–R106.
- Vimal, S. K., Ahamad, N., & Katti, D. S. (2016). A simple method for fabrication of electrospun

fibers with controlled degree of alignment having potential for nerve regeneration applications. *Materials Science and Engineering C*, 63, 616–627.

Wang, H., Kong, L., & Ziegler, G. R. (2018). Plasticization and conglutination improve the tensile strength of electrospun starch fiber mats. *Food Hydrocolloids*, 83, 393–396.

Yi, K., Fang Li, Q., Zhang, L., Li, N., Zhou, Y., Kon Ryu, S., & Guang Jin, R. (2013). Diffusion coefficients of dimethyl sulphoxide (DMSO) and H<sub>2</sub>O in pan wet spinning and its influence on morphology of nascent Polyacrylonitrile (PAN) Fiber. *Journal of Engineered Fibers and Fabrics*, 8(1), 107–113.